

Charge-density-wave transport in orthorhombic TaS₃. III. Narrow-band "noise"

A. Zettl and G. Grüner

Department of Physics, University of California, Los Angeles, Los Angeles, California 90024

(Received 12 November 1982)

Narrow-band noise measurements are reported for the linear chain Peierls semiconductor, orthorhombic TaS₃. In the nonlinear conductivity region, sharp narrow-band noise peaks are observed with several harmonics. The amplitudes of the peaks are temperature dependent, starting from zero just below the charge-density-wave (CDW) transition at $T_P \sim 215$ K, and remaining approximately constant below $T = 170$ K. Between T_P and approximately 100 K, where both the field- and the frequency-dependent conductivities suggest highly coherent response of the CDW condensate, the noise spectrum is simple (fundamental and harmonics). At low temperatures the noise spectrum becomes quite complicated, with many fundamental and harmonic peaks present, due to a loss of the transverse coherence in the material and indicative of a disordered CDW state. At intermediate temperatures a linear relationship is found between the excess CDW current and the fundamental noise frequency. Analysis in terms of coherent motion of the CDW indicates that the characteristic distance associated with the narrow-band noise is approximately equal to one CDW wavelength λ and that pinning is dominated by impurities rather than by commensurability. A comparison of the data is made with the predictions of the classical model of CDW transport and with Bardeen's theory of coherent current oscillations. The noise observations are compared to and contrasted with related measurements performed on the similar CDW material NbSe₃.

I. INTRODUCTION

The quasi-one-dimensional linear-chain compound orthorhombic TaS₃ undergoes a Peierls phase transition to a semiconducting state at $T_P = 215$ K.¹ The ground state is characterized by a gap in the single-particle excitation spectrum and by the collective charge-density-wave (CDW) mode, which in the conventional notation is written as

$$\Delta\rho(x) = A \cos(2k_F x + \phi),$$

where x refers to the chain direction, and A and ϕ are the amplitude and phase of the CDW. The period of the CDW is given by $\lambda = \pi/k_F$. In TaS₃ the associated CDW is commensurate with the underlying lattice with a period $4c$ where c is the lattice constant along the chain direction.² The highly unusual electrical transport properties in the CDW state, in particular the strongly nonlinear dc conductivity³⁻⁵ and frequency-dependent⁶⁻⁸ ac conductivity, suggest a collective charge-transport mechanism. The observed response in TaS₃ parallels closely that of NbSe₃, a related linear-chain compound which has been the prototype for CDW transport studies.⁹ Studies on the incommensurate CDW modes of

NbSe₃ have indicated that impurities will pin the CDW in place for low applied electric fields E , but that sufficiently high fields can depin the CDW and enhance the conductivity by the Fröhlich mechanism.¹⁰ In addition to nonlinear conductivity studies,⁶⁻⁸ low field ac conductivity studies¹¹ of NbSe₃ show an anomalously large dielectric constant, again indicating a collective response of the CDW mode.

In two previous publications^{12,13} (hereafter referred to as I and II), we have described the CDW response of orthorhombic TaS₃ to both dc and ac driving fields. In I we showed that below T_P (but above approximately 100 K the dc response $\sigma(E)$ is characterized by a strongly nonlinear conductivity with a well-defined threshold field E_T for the onset of nonlinear conduction. In this same temperature region the ac conductivity $\sigma(\omega)$ suggested an overdamped oscillator response when interpreted in terms of a response of a classical harmonic oscillator. Detailed analysis of both $\sigma(E)$ and $\sigma(\omega)$ gave excellent quantitative fits to the predictions of a model of CDW tunneling across a pinning gap.^{14,15} At temperatures lower than approximately 100 K the forms of $\sigma(E)$ and $\sigma(\omega)$ suggested a loss of correlation between CDW segments and an increased role played by disorder.

One of the most striking features of CDW trans-

port is the appearance of narrow-band noise in the response-power spectrum for applied dc fields exceeding the threshold E_T . The noise peaks (fundamental and several harmonics) reflect a periodic time-dependent response to a dc applied field. In this regard the notation “noise” is not appropriate; nevertheless we will use this notation to be consistent with the notation used in previous works.¹⁵ These noise observations were first made on NbSe₃ (Refs. 16–18) and were later also observed in orthorhombic TaS₃.¹⁹ In this publication we report detailed measurements of the narrow-band noise in orthorhombic TaS₃. We find that the field dependence of the peaks in the noise spectrum at intermediate temperatures suggests a linear relationship between the excess CDW current I_{CDW} and the fundamental frequency of the narrow-band noise.^{18,19} In addition, the temperature dependence of the noise spectrum suggests coherent sample response at higher temperatures and a loss of coherence between conducting chains at lower temperatures, a conclusion also reached on the basis of the field- and frequency-dependent response. We analyze our data both in terms of a classical model of CDW transport²⁰ and in terms of a recent description²¹ of coherent current oscillations in NbSe₃ where the current oscillations and associated narrow-band noise are taken to arise from the sliding of the CDW over the peaks and valleys of the potential that pins the phase of the wave. Analysis of the data indicates that the characteristic distance associated with the narrow-band noise is approximately equal to one CDW wavelength λ and that pinning is dominated by impurities rather than by commensurability.

This paper is organized as follows: In Sec. II we describe the experimental techniques used to obtain the narrow-band noise data. Section III contains the experimental results, which are discussed in Sec. IV. A comparison with NbSe₃ in Sec. V is followed by the conclusion in Sec. VI. Parts of our experiments were published earlier.¹⁹

II. EXPERIMENTAL TECHNIQUES

Orthorhombic TaS₃ crystals used in this study were from the same preparation batch as those used in $\sigma(E)$ and $\sigma(\omega)$ reported in I and II. Typical crystal dimensions before mounting were 5 mm \times 10 μ m \times 1 μ m, where the long dimension corresponds to the chain axis (c axis). We have used a two-probe mounting configuration with conductive silver paint contacts. Contact resistances were typically a few ohms, or more than 2 orders of magnitude smaller than the sample resistance at $T=200$ K. To insure a uniform sample cross section and to avoid self-

heating effects of the sample we have used a contact spacing less than 0.5 mm. This distance corresponds to that along the chain axis and it is with respect to this axis that the driving signal was applied and the response was measured. The sample was driven by a dc current source and the sample-current and time-averaged (dc) voltage response were measured using conventional digital voltmeters. By comparing the dc I - V characteristics with those obtained on similar samples with the use of a pulsed technique we have verified that sample heating effects were negligible for the highest fields reported here.

Simultaneously with the dc measurements the ac voltage response of the sample was detected and amplified with a differential broad-band amplifier developed by ourselves, with a gain of 50 and a bandwidth of 100 MHz. A short (10-cm) coaxial cable was used between the sample and amplifier to eliminate reflections or standing-wave problems. The amplifier output was then Fourier decomposed using a (1–100)-MHz spectrum analyzer. A significant improvement in the spectrum-analyzer output signal was obtained by averaging approximately 250 sweeps of the spectrum analyzer with a multichannel signal averager. Occasionally up to 2048 sweeps were recorded when the narrow-band noise amplitude was very small. A specially designed ⁴He gas-flow cryostat was used to vary the temperature. This system has a temperature accuracy of about 1 K and a stability better than 0.1 K at all temperatures.

III. EXPERIMENTAL RESULTS

Figure 1 shows the frequency spectrum of the voltage response of orthorhombic TaS₃ for various values of the applied electric voltage at $T=165$ K. The sample was actually driven from a current source and thus V represents the time-averaged dc value. Below a critical voltage V_c there is no evidence for either broad- and narrow-band noise, as shown in the upper trace of the figure. For $V > V_c$, a dominant and relatively sharp noise peak appears at frequency f_1 with harmonics of diminishing amplitude also apparent. The dominant or fundamental peak and its associated harmonics move to higher frequencies with increasing applied bias V and no upper limit on the frequency of the fundamental was observed.

Figure 2 shows the frequency spectrum for an applied dc voltage $V=1.7V_c$, or equivalently, an applied electric field $E=1.7E_c$, in greater detail. The strong and sharp fundamental noise peak is clearly seen at $f_1=10$ MHz and two higher harmonics of lesser amplitude are apparent at 20 MHz $=2f_1$ and

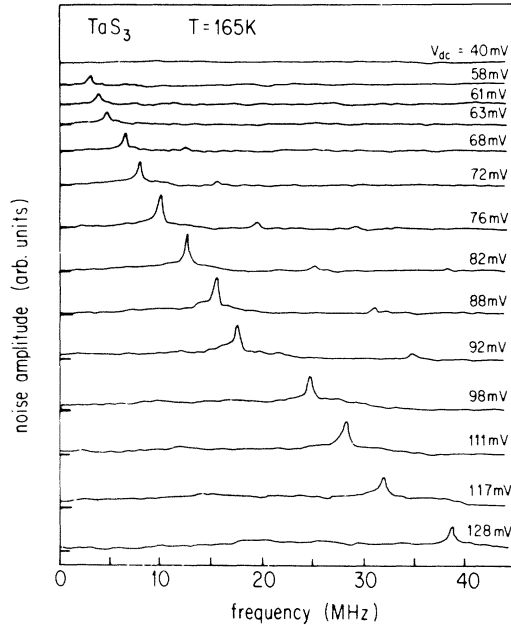


FIG. 1. Narrow-band noise spectrum of orthorhombic TaS_3 at $T=165$ K for various values of the applied dc bias voltage. Threshold voltage for the onset of nonlinear conduction is $V_T=45$ mV.

30 MHz $= 3f_1$. The dashed line indicates the baseline for zero ac response and thus a small amount of broad-band noise is observed between successive harmonics. Although there is some frequency spread near the base of the fundamental noise peak at f_1 , we find no clear evidence for subharmonics of f_1 .

The dc I - V characteristics of TaS_3 measured simultaneously with the data displayed in Fig. 1 and plotted as a normalized conductivity versus applied dc bias voltage are shown in Fig. 3. The threshold voltage for the onset of nonlinear conduction is clearly seen at $V_T=45$ mV. With the use of the measured sample length $l=0.2$ mm this corresponds to a threshold electric field $E_T=2.2$ V/cm, in good agreement with values reported in I. A detailed comparison of the noise spectrum for different applied bias fields E and the nonlinear I - V characteristics of the sample indicates that the critical field for the onset of narrow-band noise is identical to the threshold field for the onset of nonlinear conduction, i.e., $E_c=E_T$. Similar observations have been made in both CDW states of NbSe_3 .¹⁶

As can be seen from Fig. 1, the amplitudes of the fundamental frequency f_1 and its harmonics are field dependent. In the nonlinear conductivity region the peak height first smoothly increases with increasing E just above E_T . Owing to instrumental limitations we were not able to measure the noise peaks at frequencies below approximately 1 MHz. We expect, however, that near E_T the fundamental noise peak will continue to decrease smoothly in fre-

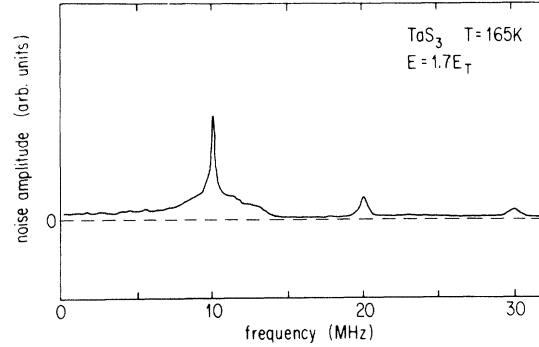


FIG. 2. Frequency spectrum of the voltage oscillations in the nonlinear conductivity region of orthorhombic TaS_3 in the coherent CDW state. Fundamental noise peak is clearly seen at 10 MHz with two higher harmonics also present. Dashed line represents the baseline for zero ac response.

quency and amplitude with decreasing applied E , approaching zero amplitude at threshold. Between approximately $2E_T$ and $3E_T$ the amplitude of the fundamental peak decreases slightly with increasing E . An extension of measurements into the high-field and -frequency limit (>100 MHz) was hampered by severe sample-heating effects.

The general appearance of the noise spectrum is

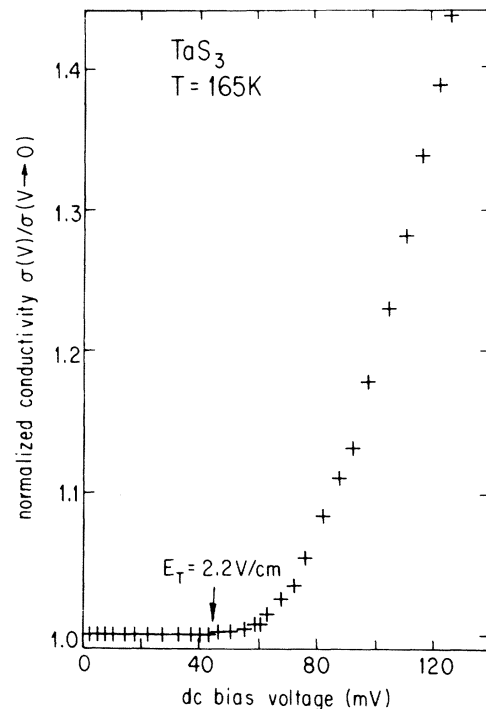


FIG. 3. Normalized dc conductivity vs applied dc bias voltage for orthorhombic TaS_3 at $T=165$ K. Threshold voltage for the onset of nonlinear conduction is indicated by the arrow. Data are for the same sample as used for Fig. 1.

strongly temperature dependent. This is shown in Fig. 4 where we have selected several frequency traces at various temperatures for a single sample. We find that the noise spectrum is most clearly defined at approximately $T = 170$ K. At this temperature f_1 and its higher harmonics are clearly seen and the peaks are quite sharp. In fact, for moderate electric field strengths the finite width (at half maximum) of the peaks appears to be instrumental. This was verified by substituting for the sample a carbon resistor driven by a frequency synthesizer which yielded a comparable peak width at half maximum. At higher temperatures the amplitude of the noise peaks in general decreases and higher harmonics are difficult to observe. Above approximately 205 K we were not able to observe any narrow-band noise component, although the conductivity is still nonlinear in this temperature region up to the phase transition at 215 K with a well-defined threshold field. At temperatures below approximately $T = 140$ K, the noise spectrum becomes rather complicated with several fundamental frequencies and harmonics present. This is shown in Fig. 5 where several frequency traces are shown for different values of the applied voltage V at $T = 140$ K. The spectrum becomes even more smeared with decreasing temperature and below approximately 90 K it becomes impossible to isolate a dominant noise peak. The complexity of the noise spectrum at lower temperatures appears to be closely related to the smearing of both

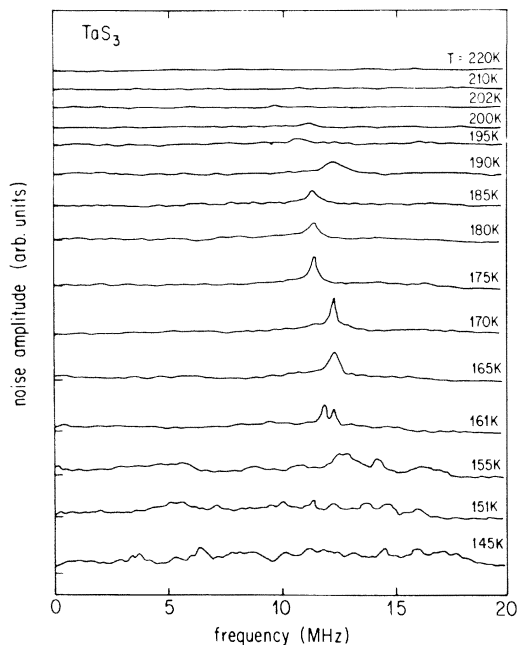


FIG. 4. Frequency spectra of the voltage oscillations in orthorhombic TaS_3 at selected temperature. Above $T_p = 215$ K no noise peaks are observed. For each temperature below T_p the dc bias field has been chosen to produce a fundamental noise peak near 12 MHz.

the dc and ac responses at low temperatures as discussed in I and II.

It is important to note that the quality of the narrow-band noise spectrum in TaS_3 is extremely sample dependent. Even for crystals from the same preparation batch a wide variety of narrow-band spectra for a given temperature is found. Some samples showed complicated spectra even at $T = 170$ K, similar in appearance to those shown in Fig. 5, which is for an average quality crystal at $T = 140$ K. A few exceptionally high quality crystals showed reasonably "clean" narrow-band spectra to about 100 K. For such crystals signal averaging of the spectrum-analyzer output was not necessary and the frequency of the fundamental noise peak could be read directly from the spectrum-analyzer cathode-ray-tube (CRT) display. The f_1 -vs- E data for such a sample at $T = 130$ K is presented in Fig. 6.

IV. DISCUSSION

In both I and II careful comparisons were made between experimental $\sigma(E)$ and $\sigma(\omega)$ data and the predictions of the classical model of CDW transport²⁰ and the quantum-mechanical-tunneling model.^{14,15} Voltage oscillations and associated

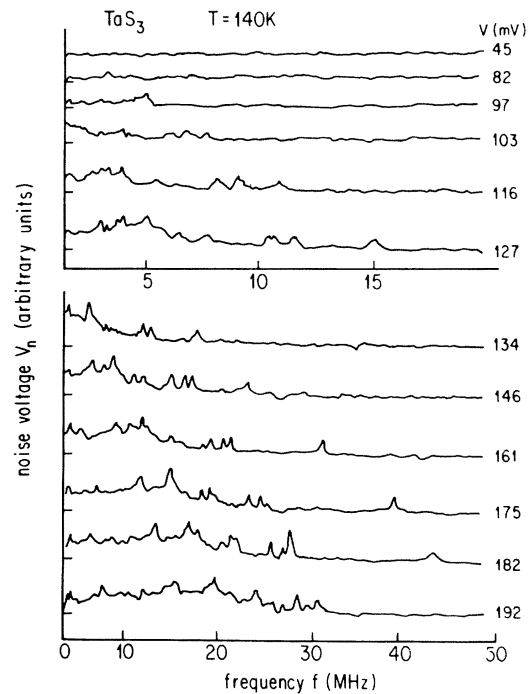


FIG. 5. Frequency spectra of the voltage oscillations in orthorhombic TaS_3 at $T = 140$ K. Threshold voltage for the onset of nonlinear conductivity is at $V_T = 75$ mV for this sample. Note the different frequency scales for the data below $V = 130$ mV.

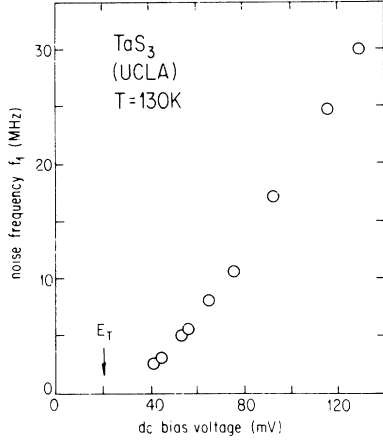


FIG. 6. Fundamental noise frequency vs applied dc bias voltage for orthorhombic TaS₃ at $T = 130$ K. Data are for a particularly good sample which produced a simple narrow-band noise spectrum even at this low temperature.

narrow-band noise in the nonlinear conductivity region are natural consequences of the classical model but follow also from arguments developed recently by Bardeen.²¹ Bardeen's theory does not depend on the details of the mechanism of the CDW but requires only that the CDW slide without dissipation over the peaks and valleys of the pinning potential. This theory should apply to the tunneling model but it is expected that a description in terms of classical CDW motion with inertia terms included will lead to a similar description.

In both descriptions, in the nonlinear conductivity region the CDW slides over the periodic pinning potential, transporting charge and giving rise to an enhanced dc conductivity. Assuming a constant effective charge for the CDW and thus a constant external driving force provided by the applied electric field E (voltage-controlled situation), the CDW velocity will vary periodically in time due to the motion of the CDW over the potential peaks and valleys. Thus the excess current provided by the sliding CDW, I_{CDW} , will contain an oscillating component. This oscillating component gives rise to the narrow-band noise at f_1 , and, because of the asymmetry of the velocity function, to higher harmonics.

Two aspects of the observed noise spectrum are of importance. First, the relative amplitude of the harmonics is related, through the time-dependent CDW velocity $v_d(t)$, to the shape of the periodic potential and to the relative importance of damping and inertia effects. Second, the dependence of the noise frequency on the applied field or on the current carried by the CDW establishes the length of the periodic

potential or the charge associated with the current oscillations.

A. Noise harmonics and amplitude

In this section we analyze the harmonic content of the narrow-band noise spectrum at intermediate temperatures ($T \sim 170$ K). We investigate how the amplitude of the observed harmonics varies with the order of the harmonic and also how the amplitude of a given harmonic varies as a function of applied electric field E .

As seen in Fig. 1, at $T = 165$ K, TaS₃ displays a reasonably clear and simple narrow-band noise spectrum with one sharp noise peak at f_1 and peaks of smaller amplitude apparent at $2f_1$ and $3f_1$. In other words, we are able to clearly resolve the first three harmonics of the coherent voltage oscillations in the sample. Careful noise measurements on NbSe₃ with the use of high-purity samples²² have revealed very similar noise spectra with up to eight harmonics observable. In I and II we discussed a classical model of CDW transport based on a phenomenological description of the pinned CDW by Lee, Rice, and Anderson.²³ This model described in a qualitative way the main features observed for the field- and frequency-dependent conductivity, i.e., the nonlinear dc conductivity $\sigma(E)$ with a sharp threshold E_T and saturation at high electric fields E , the overdamped response of $\sigma(\omega)$ with the frequency dependence extending to $\omega \rightarrow 0$, and the saturation of $\sigma(\omega)$ at high frequency ω . The model also accounts for experiments performed in the presence of ac and dc driving fields. In this model the CDW is treated as a charged classical particle of effective charge e and mass M moving in a periodic potential subject to external driving forces and to damping. In the model, for a sinusoidal potential and overdamped motion, the equation of motion is

$$\frac{1}{\tau} \frac{dx}{dt} + \frac{\omega_0^2}{Q} \sin(Qx) = \frac{eE}{M}, \quad (1)$$

where $\Gamma = M/\gamma$ with γ the damping constant, $\omega_0^2 = k/M$ where k is the restoring force constant, and $Q = 2\pi/\lambda$ where λ is the period of the pinning potential. Equation (1) is formally the same as the equation which describes the behavior of a resistively coupled Josephson junction.²⁴ The correspondence between CDW and Josephson-junction phenomena has been recognized by various groups, among them Ben-Jacob.²⁵ For $E > E_T$, Eq. (1) yields a CDW velocity

$$\frac{dx}{dt} = \frac{\frac{\tau}{2} \left[\frac{e\alpha E}{M} + \frac{\omega_0^2}{Q} \right]}{\alpha + \frac{1}{\alpha} [\cos^2(\omega t) - \sin^2(\omega t)] - 2(1 - \alpha^{-2})^{1/2} \sin(\omega t) \cos(\omega t)}, \quad (2)$$

where

$$2\omega = \left[\frac{e^2 E^2 \tau^2}{M^2} - \frac{\omega_0^4 \tau^2}{Q^2} \right]^{1/2}$$

and $\alpha = E/E_T$, with the threshold field $E_T = M\omega^2/eQ$. Equation (2) predicts a fundamental oscillation frequency

$$f_1(E) = \frac{Q\tau e}{M} (E^2 - E_T^2)^{1/2}, \quad (3)$$

with harmonics in the CDW current at

$$I_n \sim (\alpha^2 - 1)^{1/2} [\alpha - (\alpha^2 - 1)^{1/2}]^n \cos \left[n \left(\omega t + \frac{\pi}{2} + \sin^{-1} \alpha \right) \right], \quad (4)$$

with $n = 1, 2, 3, \dots$. The time-averaged CDW current density for the entire sample is given by

$$J_{\text{CDW}} = \frac{n_c^2 \tau}{ME} (E^2 - E_T^2)^{1/2}, \quad (5)$$

where n_c is the density of electrons condensed in the CDW state. Equation (5) leads to a simple relation between the CDW current density and the fundamental noise frequency,

$$\frac{J_{\text{CDW}}}{f_1} = n_c(T)e\lambda. \quad (6)$$

From Eq. (4) we see that the amplitude of higher harmonics decreases with increasing n . In Fig. 7 we show the narrow-band noise spectrum of TaS₃ at $T = 165$ K and $E = 1.7E_T$. The solid line in the figure is Eq. (4) normalized to the fundamental frequency peak. Although this fit appears to be quite good, it should be noted that the calculated relative amplitude of the harmonics is a rather sensitive function of $\alpha = E/E_T$, and that for increasing E the amplitudes of the higher harmonics are predicted to decrease quite rapidly as the time-dependent current approaches a sinusoidal function. This is in contrast to experimental observations which indicate that the relative amplitudes of the noise harmonics are rather insensitive to the magnitude of the applied field.

In an electrical analog model²² of CDW response in the nonlinear conductivity region the CDW's are represented by relaxation oscillators which lock together in phase due to a weak resistive or capacitive coupling. The resulting waveform of the coupled system is periodic in time and can be rich in harmonics. For a sawtooth waveform, successive har-

monics fall off like $1/n$, and for a triangular waveform, they fall off like $1/n^2$. In Fig. 7 we have plotted both the $1/n$ and $1/n^2$ decays. It is apparent that the experimental data lie intermediate to the $1/n$ and $1/n^2$ decays, a result also obtained for narrow-band noise measurements²² on NbSe₃. A detailed fit to the TaS₃ data yields a $1/n^{1.7}$ decay, but we do not regard this exponent as significant.

As can be seen from Fig. 1, the amplitude of the fundamental noise peak at f_1 is field dependent. For $E < E_T$, the amplitude of the noise is zero, as

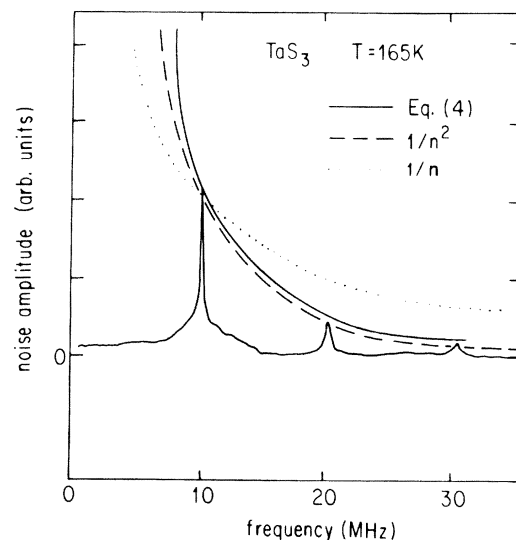


FIG. 7. Narrow-band noise spectrum for orthorhombic TaS₃ at $T = 165$ K. Amplitude decay of higher harmonics is close to a $1/n^2$ behavior as indicated by the dashed line in the figure. Solid line is a fit to the classical-model prediction, Eq. (4). Dotted line shows a $1/n$ falloff.

expected for a pinned CDW. For $E > E_T$, the amplitude of the fundamental first increases smoothly with increasing E and then slightly decreases for fields greater than approximately $2E_T$. Setting $n = 1$ in Eq. (4), which then gives the amplitude of the first harmonic in the classical model,²⁰ we obtain

$$A_1(E) \sim \left[\left(\frac{E}{E_T} \right)^2 - 1 \right]^{1/2} \left\{ \frac{E}{E_T} - \left[\left(\frac{E}{E_T} \right)^2 - 1 \right]^{1/2} \right\}. \quad (7)$$

A similar expression has been obtained recently by Monceau *et al.*²⁶ with the use of the same model as proposed in Ref. 20. In Fig. 8 we have plotted the amplitude of the fundamental noise peak of TaS₃ as a function of E with the use of the data of Fig. 1. The full line in Fig. 8 is Eq. (7) normalized to $A_1(E = 80 \text{ mV}) = 3$. It is apparent that the amplitude of the fundamental increases much slower with increasing electric field than that predicted by the classical model. The rapid increase predicted by the model is related to the rapid increase of I_{CDW} above threshold and to the divergence of the differential conductivity dI_{CDW}/dE as E approaches E_T from above. As discussed in I, this divergence has not been observed by experiment where I_{CDW} is found to increase more slowly with increasing E above E_T , with a functional form suggestive of tunneling phenomena.¹⁴ An amplitude of the fundamental proportional to the observed I_{CDW} would lead to the measured smooth increase of A_1 as seen in Fig. 8.

Although the scatter of the experimental data is fairly large in Fig. 8, it appears that in the high-electric-field limit the amplitude of the fundamental decrease with increasing E , in contrast to the prediction of Eq. (6) and also in disagreement with an overdamped response in the current-carrying state for any form of the periodic potential. This may be related to a finite-inertia effect of the CDW which is not included in Eq. (1). A classical harmonic oscillator with inertia described as

$$\frac{d^2x}{dt^2} + \frac{1}{\tau} \frac{dx}{dt} + \frac{\omega_0^2}{Q} \sin(Qx) = \frac{eE}{M} \quad (8)$$

leads to a time-dependent current; however, in the high-electric-field limit the amplitude of the current oscillations decreases and is inversely proportional to the CDW current I_{CDW} . Assuming that the functional form of the time dependence depends only weakly on E , one expects $A_1(E)$ to decrease with increasing applied bias voltage, as observed experimentally.

Arguments which also emphasize the role in an inertia term have recently been developed by Bardeen.²¹ In a description of the coherent current os-

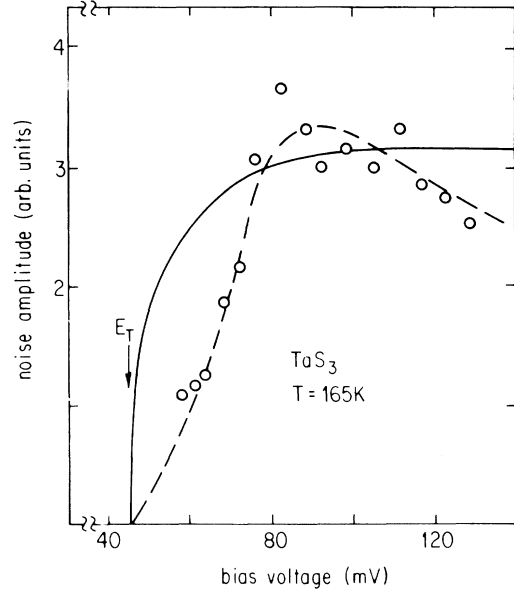


FIG. 8. Amplitude of the fundamental noise peak vs applied dc bias voltage for orthorhombic TaS₃ at $T = 165$ K. Threshold field is indicated by an arrow. Solid line is the prediction of the classical model (neglecting inertial effects), Eq. (7). Dashed line is a guide to the eye for the experimental data.

cillations in NbSe₃ it was suggested that the CDW moves adiabatically over the periodic pinning potential $V(\phi)$ in such a way that the total energy of the wave, kinetic plus potential, is constant. The CDW velocity is composed of a time-independent and a time-dependent component,

$$v = v_d + v_1(\phi), \quad (9)$$

where v_d represents the time average velocity, v_1 is the oscillating component of the velocity, and ϕ is the phase of the CDW relative to a potential minimum. The assumption that the sum of the kinetic and potential energy of the moving CDW is conserved in the large-velocity ($v_d \gg v_1$) limit leads one to obtain for the oscillating component of the current ΔI ,

$$\Delta I \times I_{\text{CDW}} = \frac{-V(\phi)}{m^* n_c^2 e^2 A^{-2}} = \text{const}, \quad (10)$$

where m^* is the effective mass of the CDW, n_c is the density of electrons condensed in the CDW state, and A is the cross-sectional area of the sample. Here the sample is assumed to be driven by a voltage source. Equation (10) predicts that in the high-field limit the amplitude of the current oscillations decreases with increasing I_{CDW} , i.e., with increasing E . The amplitude of the coherent current or voltage oscillations is given by the inverse Fourier transform of the noise spectrum. If the dependence of E on the higher harmonics in the noise spectrum is the

same as that of the fundamental frequency, we can approximate the amplitude of the oscillations by A_1 , the amplitude of the fundamental noise peak. We see from Fig. 8 that in the high-field limit, A_1 , and thus ΔI , appears to decrease slightly with increasing E , in qualitative agreement with the predictions of Eq. (10). Owing to sample-heating effects, however, we were not able to extend our experiments to higher electric fields where Eq. (12) could be tested quantitatively.

B. Current-frequency relation

In this section we analyze the relation between the fundamental noise frequency f_1 and the excess CDW current I_{CDW} . We shall proceed with the assumption that the narrow-band noise arises from the CDW sliding over the periodic pinning potential and that the fundamental noise frequency f_1 is proportional to the time-averaged CDW drift velocity v_d . If λ represents the period of the potential, then $f_1 = v_d/\lambda$. Since $I_{CDW} = n_c e v_d A$, Eq. (6) follows. Equation (6) predicts that for constant n_c , e , λ , and A , f_1 is directly proportional to I_{CDW} . This linear relation between the noise frequency and CDW current was first proposed by Monceau *et al.*¹⁸ on experimental grounds for NbSe₃. It is also predicted by the classical model.²⁰ Studies of NbSe₃ have verified the linear relation up to $f_1 = 100$ MHz.²²

Figure 9 shows the fundamental noise frequency f_1 vs I_{CDW} for TaS₃ at $T = 130$ K. Experimental data shown in the figure were extracted from Fig. 6, which was obtained on an exceptionally good sample. I_{CDW} is defined by $I_{CDW} = I - V/R_0$ where I is the measured dc sample current, V is the dc sample voltage, and R_0 is the low-field (Ohmic) sample resistance. It is clear that a linear relation is found over a reasonably wide frequency range. From Eq. (9) and the measured slope $I_{CDW}/f_1 = 45 \mu\text{A MHz}^{-1}$, the characteristic distance λ can be determined. From the measured sample length, the sample resistance, and the room-temperature conductivity $\sigma = 2.6 \times 10^3 \Omega^{-1} \text{cm}^{-1}$, we obtain a cross-sectional area $A = 9.62 \times 10^{-7} \text{cm}^2$. n_c can be determined from the published² lattice parameters and we find a value $n(T=0) = 2.6 \times 10^{21}$. This value is easily corrected for finite-temperature effects with the use of the temperature dependence of the CDW order parameter as determined from x-ray studies.³ We thus obtain $n(T=130 \text{ K}) = 1.9 \times 10^{21}$ electrons/cm³. Equation (6) then yields $\lambda = 13.26 \text{ \AA}$, in excellent agreement with the CDW wavelength $\lambda_{CDW} = 13.3 \text{ \AA}$. It thus appears that although orthorhombic TaS₃ is a commensurate system the CDW pinning is dominated by impurities. This result is further substantiated by studies of TaS₃ crystals with varying amounts of substitutional impuri-

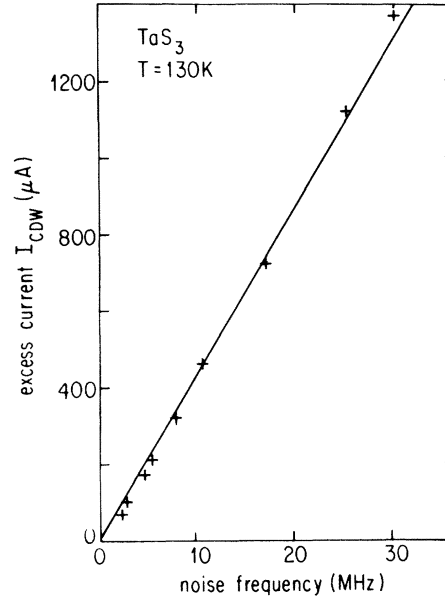


FIG. 9. Excess CDW current I_{CDW} vs frequency f_1 of the fundamental noise peak in orthorhombic TaS₃ at $T = 130$ K. Data correspond to that shown in Fig. 6. Linear relation yields strong support for Eq. (6).

ties in which the threshold field for the onset of nonlinear conduction was found to increase dramatically with an increasing concentration of impurities.²⁷

Since the density of electrons per chain condensed in the CDW state is given by $n_c = \pi/k_F$, Eq. (6) can also be written as

$$\frac{I_{CDW}}{f_1} (\text{per chain}) = 2e \frac{n_c(T)}{n_c(0)}. \quad (11)$$

It has recently been suggested that a moving soliton lattice²⁸ with a fractional²⁹ soliton charge $e/2$ is responsible for the oscillating current. In this case Eq. (11) must be rewritten as

$$\frac{I_{\text{excess}}}{f_1} (\text{per chain}) = \frac{e}{2} \frac{n_c(T)}{n_c(0)}. \quad (12)$$

The same result, i.e., Eq. (12), is obtained³⁰ in the CDW case if the oscillation frequency corresponds to a displacement of the CDW by one lattice constant $a_0 = \lambda/4$. The analysis of I_{CDW}/f_1 discussed previously for TaS₃ indicates that for $T=0$, I_{CDW}/f_1 (per chain) is $1.8 \pm 0.5e$, in close agreement with the predictions of Eq. (11), supporting strongly that charge transport is by sliding CDW's.

We also mention that a linear relation between f_1 and I_{CDW} is not always observed in TaS₃ but deviations from such behavior are due to an inhomogeneous cross section of the specimen or inhomogeneous current injection through the silver paint contacts. A complicated noise spectrum is usually

associated with nonlinear I_{CDW} -vs- f_1 curves. This is shown in Fig. 9 where we have plotted f_1 vs I_{CDW} for a relatively poor sample at $T=170$ K. Although f_1 appears to start from zero at $I_{CDW}=0$, the slope dI_{CDW}/df_1 is not constant. Only in the high-field limit does this slope approach a constant value. We suggest that the increase in dI_{CDW}/df_1 with increasing I_{CDW} reflects an inhomogeneous current density within the sample. As E is increased above E_T more and more CDW domains in the sample become mobile and contribute to I_{CDW} . For such ill-defined samples we have also observed a fair amount of broad-band noise along with abnormally wide frequency widths for the fundamental noise peaks. Further evidence for an inhomogeneous current distribution is the form of the dc conductivity just above threshold. Although at moderate temperatures ($T\sim 170$ K) a reasonably well-defined threshold field E_T is observed for these samples, the conductivity increase just above E_T is very gradual, in contrast to the relatively sharp increase in the conductivity above E_T found in high-purity NbSe₃ samples. We note that even for NbSe₃ samples nonlinear relations have been found²⁶ between I_{CDW} and f_1 with a functional form similar to that shown in Fig. 9. For high-quality NbSe₃ samples, however, a linear relation is always observed.^{21,31}

From Eq. (6) we see that I_{CDW}/f_1 gives a direct measure of $n_c(T)$, the density of electrons condensed in the CDW state. Using data at various temperatures similar to those shown in Fig. 7 we have evaluated I_{CDW}/f_1 as a function of temperature. The results are shown in Fig. 10. We find an increasing n_c with decreasing temperature below the transition, as expected for the temperature-dependent CDW order parameter $\Delta(T)$. Figure 10 also shows $\Delta(T)$ as evaluated from conductivity measurements,³² x-ray studies,² and thermopower measurements.³³ The dc conductivity determination of $\Delta(T)$ is from the work of Ido *et al.*³² where $\Delta(T)$ was calculated from the low-field (Ohmic) dc conductivity with the use of the expression

$$\sigma_{dc}(T) = \sigma_0 \exp \left[\frac{-\Delta(T)}{k_B T} \right].$$

The x-ray data represent the amplitude of the superlattice peaks as measured by Tsutumi *et al.*² In the analysis of the thermoelectric power S we have used the relation

$$S \sim (\mu_e - \mu_n) \frac{\Delta(T)}{k_B T},$$

where S is the absolute thermoelectric power and the μ_e and μ_n refer to electron and hole mobilities, respectively. Thus, assuming that the mobilities are

temperature independent, $\Delta(T) \sim S k_B T$. In determining S we have used TaS₃ crystals from the same preparation batch as was used for the narrow-band noise measurements and also for the studies reported in I and II. Figure 10 shows a remarkable agreement between $\Delta(T)$ as evaluated from the analysis of the narrow-band noise data and that evaluated from structural measurements and from experiments which are sensitive to the number of uncondensed electrons. A similar conclusion was recently reached for NbSe₃.²¹ We also note that the temperature dependence of Δ is weaker than that given by the Bardeen-Cooper-Schrieffer (BCS) form. This may be due to deviations from mean-field behavior due to the highly anisotropic electronic structure of TaS₃.

C. Temperature dependence of the noise spectrum

As discussed in I and II the disappearance of a sharp threshold field and the slow rise of the frequency-dependent conductivity at low temperatures (somewhat below 130 K) is indicative of a loss of coherent CDW response. The noise measurements provide direct evidence for this conjecture: While only one dominant noise peak and its harmonics are observed at high temperatures, somewhat below 130 K the noise spectrum becomes rather complicated. Although the amplitude of the noise remains high at low temperatures, the width of the peaks increases dramatically. Moreover, we can no longer clearly distinguish the dominant noise peak at f_1 . Rather, several large peaks appear, each with

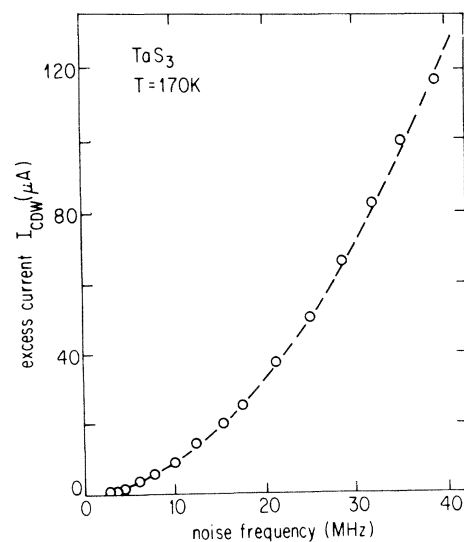


FIG. 10. Excess CDW current I_{CDW} vs frequency f_1 of the fundamental noise peak in orthorhombic TaS₃ at $T=170$ K. Data are for a rather poor sample and the nonlinear relation found indicates an inhomogeneous current density within the sample.

corresponding higher harmonics. The situation worsens with lowering temperature and at 90 K we find that the noise pattern resembles more a high level of broad-band noise with varying amplitude than clear narrow-band noise peaks. However, for a given field E , the noise amplitude above a certain frequency is very small. This “frequency front” for the noise amplitude moves to higher frequencies with increasing E . We suggest that these low-temperature effects are the result of a loss of phase coherence between the response of different CDW segments. In I we found that at low temperatures the threshold field for the onset of nonlinear conduction became less well defined and below 100 K the nonlinearity extended to $E \rightarrow 0$. We called this region a disordered CDW state in which the CDW segments responded individually to give a smeared response. In II we found that the low-temperature response was characterized by an ac conductivity $\sigma(\omega) \sim \omega^\beta$ characteristic of a random system, again arguing for the loss of a coherent CDW response. The loss of both transverse coupling between chains and longitudinal coherence in TaS₃ at lower temperatures may in part be due to the semiconducting nature of the sample. At lower temperatures fewer and fewer normal electrons are excited across the Peirels gap and thus the screening effect of the normal carriers of the electric field distribution is reduced with decreasing temperature. The result is a nonuniform electric field within the sample due to electric fields which may build up at grain boundaries, dislocations, and impurities. These effects become especially pronounced in a material with fibrous morphology such as TaS₃, where inhomogeneous electric fields can lead to different current densities within the sample with each current path producing its own narrow-band noise peak. Thus at low temperatures noise should still be observed but the dominant frequency will be ill defined, as observed.

In the coherent CDW region between approximately 130 K and T_P the long-range phase coherence associated with the current-carrying condensate is directly confirmed by the clean-noise spectrum, as discussed before. Concerning the temperature dependence in this temperature region two effects appear to be important. First, the intensity of the noise peaks strongly decreases with increasing temperature, and second, we also find a broadening of the noise peaks with increasing temperature. The strong decrease of the noise amplitude with increasing temperature appears to have two major sources. First, due to the semiconducting nature of TaS₃ in this temperature region the sample resistance is strongly temperature dependent. From the relation $\Delta V = \Delta I R$, where ΔV is the observed oscillation

voltage amplitude, ΔI is the oscillating current amplitude, and R is the sample resistance, one expects ΔV to decrease with decreasing R for fixed ΔI . Since R decreases with increasing temperature a decreasing noise amplitude is expected with increasing temperature. The second source for the decreasing amplitude is the decrease in ΔI itself due to the temperature dependence of n_c , the density of electrons condensed in the CDW mode. As T approaches T_P from below, n_c falls smoothly to zero, as can be inferred from the data in Fig. 11. The sum of the two contributions thus leads to a noise amplitude which strongly decreases with increasing temperature falling to zero at T_P , in agreement with the experimental results.

As can be seen from the data of Fig. 1, the decrease in noise amplitude with increasing temperature above 170 K is accompanied by a slight broadening of the noise peaks, i.e., a drop in the quality factor. The broadening appears to reflect the decrease in the CDW order parameter, i.e., a weakening of the three-dimensional (3D) coherence in the material as T approaches T_P . Just below the transition, both the amplitude of the noise peaks and the quality factor should smoothly approach zero, as indicated by the experimental results. We remark that a similar broadening of the noise peaks in NbSe₃ has been observed near the CDW transition temperature.²⁶

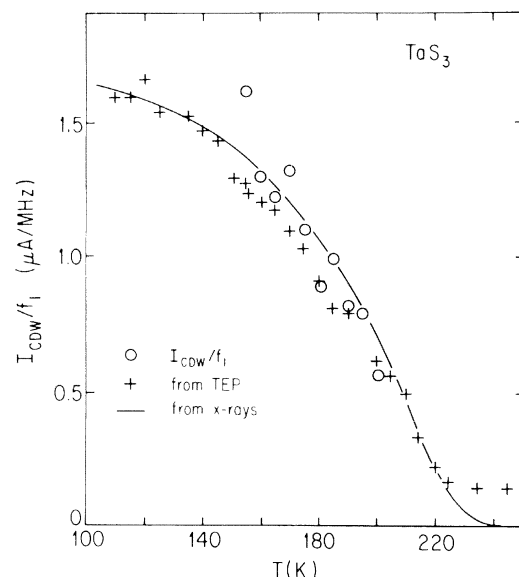


FIG. 11. Ratio of the excess CDW current I_{CDW} to the fundamental noise frequency f_1 at various temperatures for orthorhombic TaS₃. In all cases $f_1 = 12$ MHz. Ratio reflects n_c the density of electrons condensed in the CDW state [see Eq. (6)]. Crosses (+) and solid line reflect the CDW order parameter as determined from the thermoelectric power and x-ray diffraction studies (see text). CDW transition temperature is indicated by an arrow.

V. COMPARISON WITH NbSe₃

Both orthorhombic TaS₃ and NbSe₃ undergo Peierls transitions to CDW states with nonlinear conductivity and associated narrow-band noise apparent in the CDW regions. In this section we compare and contrast the observed narrow-band noise spectra of TaS₃ and NbSe₃. We suggest that the lower effective dimensionality of TaS₃ plays an important role in the spectral purity of its coherent current oscillations.

In Sec. IV we argued that although the CDW in orthorhombic TaS₃ appears to be commensurate with the underlying lattice, pinning is due to impurities. Further evidence for impurity pinning is the low threshold field $E_T \sim 0.3$ V/cm at $T = 170$ K found recently for high-quality samples.²⁷ Thus the situation is similar to that in NbSe₃ where the incommensurate CDW is pinned by impurities.^{34,35} A major difference between TaS₃ and NbSe₃ is the effective dimensionality of the system. The one-dimensional character of TaS₃ leads to a complete destruction of the Fermi surface at T_P and thus to a semiconducting state below the transition. In contrast, NbSe₃ remains metallic below the Peierls transitions, indicating that only part of the Fermi surface is removed. Hence in NbSe₃ the CDW is accompanied by a substantial number of single-particle carriers even at low temperatures. In contrast, the semiconducting nature of TaS₃ leads to a concentration of single-particle carriers which goes to zero at $T \rightarrow 0$.

The more one-dimensional nature of TaS₃ is due to the relatively small interchain coupling provided by the sulfur atoms on neighboring chains. A small interchain coupling often leads to multiple crystallographic phases for a material as exemplified by the orthorhombic and monoclinic structures of TaS₃.³⁶ Multiple phases for TaS₃ can even occur within a single needle.

At intermediate temperature the narrow-band noise spectrum in TaS₃ is very similar to that observed in NbSe₃ with the amplitude of the harmonics decreasing approximately²² as $1/n^{1.5}$. Studies of NbSe₃ samples have yielded^{18,21} a linear relationship between I_{CDW} and f_1 , consistent with the linear relationship found for high-quality TaS₃ samples. Various TaS₃ crystals have shown a nonlinear relationship between I_{CDW} and f_1 with a functional form similar to that obtained for some NbSe₃ crystals. At low temperatures the noise spectrum for TaS₃ becomes quite complicated with many noise peaks apparent. This is a direct reflection of the weak transverse coupling between chains and the freezing out of normal carriers which homogenize the electric field and current density. Owing to the

sensitivity of f_1 on the excess current density, TaS₃ samples with nonuniform cross sections will give a complicated noise spectrum even at high temperatures. We have found that very short samples with uniform cross sections give the clearest noise spectra, in agreement with the above discussion. We also note that NbSe₃ samples with obvious physical defects such as stranding near the contacts or nonuniform cross-sectional areas show noise spectra quite similar to those of TaS₃ at lower temperatures.

It is worthwhile to remark that the absolute narrow-band noise amplitude in orthorhombic TaS₃ is approximately 100 times smaller than that observed in NbSe₃. However, the relevant parameter in this case is not the height of the peaks, but rather the integrated noise intensity. It is easy to see that the slight frequency spreading near the base of the narrow-band noise peaks, as shown in Fig. 2, contributes significantly to the integrated noise intensity in TaS₃ and we find that the overall observations in TaS₃ are entirely consistent with those made on NbSe₃. The higher level of broad-band noise found in TaS₃ most probably reflects the lack of phase coherence between CDW domains, again due to the relatively high anisotropy of the TaS₃ crystals.

VI. CONCLUSION

In this report we have discussed the narrow-band noise spectrum of the linear-chain compound orthorhombic TaS₃. Above the Peierls transition temperature $T_P \sim 215$ K we see no evidence for narrow-band noise, while below T_P we see noise only for $E > E_T$ where E_T corresponds to the threshold field for the onset of nonlinear dc conduction. The amplitude of the narrow-band noise peaks decreases with increasing temperature above $T = 170$ K, falling to zero just below the transition. At temperatures near $T = 170$ K the noise peaks are sharp and well defined with one dominant peak at f_1 and higher harmonics of lesser amplitude present. At lower temperatures the amplitude of the noise peaks decreases slightly and the noise spectrum gradually becomes more complex with decreasing temperature. At low temperatures we are not able to clearly isolate a dominant noise peak, and the response indicates a loss of transverse coherence between conducting chains and an inhomogeneous current distribution within the sample.

At intermediate temperatures and for high-quality samples, f_1 is directly proportional to the excess CDW current I_{CDW} . The amplitudes and frequency dependence of the narrow-band noise peaks are in general agreement with the classical model of CDW transport. The amplitude data however indicates that an inertia term may be important for the de-

pinned CDW. Analysis of the $I_{\text{CDW-vs-}f_1}$ data indicates that the characteristic distance associated with the narrow-band noise is one CDW wavelength λ . In the high-field limit the amplitude of the voltage oscillations is in qualitative agreement with a description on narrow-band noise given for NbSe₃ where the CDW moves adiabatically over the pinning potential. Using the relation between I_{CDW} and f_1 we have evaluated n_c , the density of electrons condensed in the CDW mode. This value is in agreement with the CDW order parameter as determined from other transport and x-ray studies.

The narrow-band noise observations presented here, along with the field- and frequency-dependent response described in I and II, give strong evidence for a collective CDW transport mechanism in TaS₃. We note, finally, that the observation of the highly coherent response, which implies long-range phase coherence in the current-carrying charge density state is perhaps the most fundamental unexplained

feature of the CDW transport phenomena. In both NbSe₃ and TaS₃ the CDW is pinned by impurities, most probably through local deformations of the CDW. Models which account for pinning by impurities do not reproduce the highly coherent response, while models which lead to macroscopic phase coherence treat the pinning effects in a phenomenological way.^{37,38}

ACKNOWLEDGMENTS

We thank W. G. Clark, John Bardeen, T. Holstein, and M. Weger for useful discussions, and A. H. Thompson for providing the TaS₃ samples used in this study. We also thank A. Wong and G. di-Monte for the use of their spectrum analyzer. This work was supported in part by the National Science Foundation (NSF) under Grant No. DMR-81-0385. One of us (A.Z.) acknowledges support from an IBM fellowship.

-
- ¹T. Sambongi, T. Tsutsumi, Y. Shiodak, M. Yamamoto, K. Yamaya, and Y. Abe, *Solid State Commun.* **22**, 729 (1977).
- ²K. Tsutsumi, T. Sambongi, S. Kagoshima, and T. Ishiguro, *J. Phys. Soc. Jpn.* **44**, 1735 (1978).
- ³T. Takoshima, M. Ido, K. Tsutsumi, T. Sambongi, S. Honma, K. Yamaya, and Y. Abe, *Solid State Commun.* **35**, 911 (1980).
- ⁴A. H. Thompson, A. Zettl, and G. Grüner, *Phys. Rev. Lett.* **47**, 64 (1981).
- ⁵A. Zettl, G. Grüner, and A. H. Thompson, *Solid State Commun.* **39**, 899 (1981).
- ⁶C. M. Jackson, A. Zettl, G. Grüner, and A. H. Thompson, *Solid State Commun.* **39**, 531 (1981).
- ⁷A. Zettl and G. Grüner, *Phys. Rev. B* **25**, 2081 (1982).
- ⁸N. P. Ong, G. X. Tessema, G. Verma, J. C. Eckert, J. Savage, and S. K. Khanna, *Mol. Cryst. Liq. Cryst.* **81**, 41 (1982). G. Verma, N. P. Ong, S. K. Khanna, J. C. Eckert, and J. W. Savage (unpublished).
- ⁹For a review of the properties of NbSe₃, see R. M. Fleming, in *Physics in One Dimension*, Vol. 23 of *Springer Series in Solid State Sciences*, edited by J. Bernasconi and T. Schneider (Springer, Berlin, 1981); N. P. Ong, *Can. J. Phys.*, **60**, 757, (1982); P. Monceau, *Physica* **110B+C**, 1890 (1982); G. Grüner, *Comments Solid State Phys.* **10**, 183 (1983).
- ¹⁰H. Frölich, *Proc. R. Soc. London Ser. A* **223**, 296 (1954).
- ¹¹G. Grüner, L. C. Tippie, J. Sanny, W. G. Clark, and N. P. Ong, *Phys. Rev. Lett.* **45**, 935 (1980); S. W. Longcor and P. M. Portis, *Bull. Am. Phys. Soc.* **25**, 340 (1981).
- ¹²A. Zettl, G. Grüner, and A. H. Thompson, *Phys. Rev. B* **26**, 5760 (1982).
- ¹³A. Zettl, C. M. Jackson, and G. Grüner, *Phys. Rev. B* **26**, 5773 (1982).
- ¹⁴John Bardeen, *Phys. Rev. Lett.* **42**, 1498 (1979); **45**, 1978 (1980).
- ¹⁵John Bardeen, *Mol. Cryst. Liq. Cryst.* **82**, 1 (1982).
- ¹⁶R. M. Fleming and C. C. Grimes, *Phys. Rev. Lett.* **42**, 1423 (1979); R. M. Fleming, *Phys. Rev. B* **22**, 5606 (1980).
- ¹⁷N. P. Ong and C. M. Gould, *Solid State Commun.* **37**, 25 (1981).
- ¹⁸P. Monceau, J. Richard, and M. Renard, *Phys. Rev. Lett.* **45**, 43 (1980).
- ¹⁹G. Grüner, A. Zettl, W. G. Clark, and A. H. Thompson, *Phys. Rev. B* **23**, 6813 (1981).
- ²⁰G. Grüner, A. Zawadowski, and P. M. Chaikin, *Phys. Rev. Lett.* **46**, 511 (1981).
- ²¹John Bardeen, E. Ben-Jacob, A. Zettl, and G. Grüner, *Phys. Rev. Lett.* **49**, 492 (1982).
- ²²M. Weger, G. Grüner, and W. G. Clark, *Solid State Commun.* **35**, 243 (1980), and (in press).
- ²³P. A. Lee, T. M. Rice, and P. W. Anderson, *Solid State Commun.* **14**, 703 (1974).
- ²⁴See, for example, P. E. Lindelof, *Rep. Prog. Phys.* **44**, 949 (1981).
- ²⁵E. Ben-Jacob (unpublished).
- ²⁶P. Monceau, J. Richard, and M. Renard, *Phys. Rev. B* **25**, 931 (1982); **25**, 948 (1982).
- ²⁷Pei Ling Hsieh, A. Janossy, and G. Grüner (unpublished).
- ²⁸Per Bak, *Phys. Rev. Lett.* **48**, 692 (1982).
- ²⁹W. P. Su and J. R. Schrieffer, *Phys. Rev. Lett.* **46**, 741 (1981); R. E. Prange, *Phys. Rev. B* **26**, 991 (1982).
- ³⁰M. Weger and B. Horowitz, *Solid State Commun.* **43**, 583 (1962).
- ³¹A. Zettl and G. Grüner (unpublished).

- ³²M. Ido, K. Tsutsumi, T. Sambongi, and N. Mori, *Solid State Commun.* 29, 399 (1979).
- ³³Pei-Ling Hsieh, A. Zettl, and G. Grüner (unpublished).
- ³⁴J. W. Brill, N. P. Ong, J. C. Eckert, J. W. Savage, S. K. Khanna, and R. B. Somoano, *Phys. Rev. B* 23, 1517 (1981).
- ³⁵W. W. Fuller, G. Grüner, P. M. Chaikin, and N. P. Ong, *Phys. Rev. B* 23, 6259 (1981).
- ³⁶C. Rocau, R. Aryoles, P. Monceau, L. Guemas, A. Meercchant, and J. Rouxel, *Phys. Status Solidi A* 62, 483 (1980).
- ³⁷P. A. Lee and T. M. Rice, *Phys. Rev. B* 19, 3970 (1979).
- ³⁸L. Sneddon, M. C. Cross, and D. S. Fisher, *Phys. Rev. Lett.* 49, 292 (1982).